AD_____

Award Number: W81XWH-13-1-0125

TITLE: Imaging Prostate Cancer with Positron Emission Tomography

PRINCIPAL INVESTIGATOR: Wadas, Thaddeus J.

CONTRACTING ORGANIZATION: Wake Forest University, WINSTON-SALEM, NC 27157

REPORT DATE: July 2014

TYPE OF REPORT: Annual

PREPARED FOR: U.S. Army Medical Research and Materiel Command
Fort Detrick, Maryland 21702-5012

DISTRIBUTION STATEMENT: Approved for Public Release;
Distribution Unlimited

The views, opinions and/or findings contained in this report are those of the author(s) and should not be construed as an official Department of the Army position, policy or decision unless so designated by other documentation.

# REPORT DOCUMENTATION PAGE

*Form Approved*
*OMB No. 0704-0188*

Public reporting burden for this collection of information is estimated to average 1 hour per response, including the time for reviewing instructions, searching existing data sources, gathering and maintaining the data needed, and completing and reviewing this collection of information. Send comments regarding this burden estimate or any other aspect of this collection of information, including suggestions for reducing this burden to Department of Defense, Washington Headquarters Services, Directorate for Information Operations and Reports (0704-0188), 1215 Jefferson Davis Highway, Suite 1204, Arlington, VA 22202-4302. Respondents should be aware that notwithstanding any other provision of law, no person shall be subject to any penalty for failing to comply with a collection of information if it does not display a currently valid OMB control number. **PLEASE DO NOT RETURN YOUR FORM TO THE ABOVE ADDRESS.**

| 1. REPORT DATE | 2. REPORT TYPE | 3. DATES COVERED |
|---|---|---|
| July 2014 | Annual | 01 Sept 2013-31 Aug 2014 |

**4. TITLE AND SUBTITLE**
Imaging Prostate Cancer with Positron Emission Tomography

**5a. CONTRACT NUMBER**
**5b. GRANT NUMBER**
W81XWH-13-1-0125
**5c. PROGRAM ELEMENT NUMBER**

**6. AUTHOR(S)**
Wadas, Thaddeus J. Ph.D.

E-Mail: twadas@wakehealth.edu

**5d. PROJECT NUMBER**
**5e. TASK NUMBER**
**5f. WORK UNIT NUMBER**

**7. PERFORMING ORGANIZATION NAME(S) AND ADDRESS(ES)**
Wake Forest University

Winston-Salem, NC 27157

**8. PERFORMING ORGANIZATION REPORT NUMBER**

**9. SPONSORING / MONITORING AGENCY NAME(S) AND ADDRESS(ES)**
U.S. Army Medical Research and Materiel Command
Fort Detrick, Maryland 21702-5012

**10. SPONSOR/MONITOR'S ACRONYM(S)**
**11. SPONSOR/MONITOR'S REPORT NUMBER(S)**

**12. DISTRIBUTION / AVAILABILITY STATEMENT**
Approved for Public Release; Distribution Unlimited

**13. SUPPLEMENTARY NOTES**

**14. ABSTRACT**

Tumors associated fibroblasts (TAFs) represent a major component of a PCa tumor, and play a critical role in tumor development. The purpose of this proposal is to utilize fibroblast activation protein alpha (FAP) expression on TAFs within the tumor stroma for the diagnostic imaging of PCa using novel radiopharmaceuticals and innovative multimodal imaging platforms. The scope of this proposal is to develop peptide based radiopharmaceuticals and evaluate them as PET imaging agents in preclinical animal models of prostate cancer, which demonstrate TAF involvement. This progress report describes the completed synthesis of these peptide ligands, their radiosynthesis with copper-64 and an evaluation of their stability in human serum. A second goal achieved during the current funding period was the development of fibroblast based cell lines, which stably express eGFP and FAP. Ongoing experiments are focused on the *in vitro* and *in vivo* evaluation of each radiopharmaceutical and on understanding the growth characteristics of each transfected cell line *in vivo*.

**15. SUBJECT TERMS**
PET, Prostate Cancer, FAP, molecular imaging, peptide, copper-64

| 16. SECURITY CLASSIFICATION OF: | | | 17. LIMITATION OF ABSTRACT | 18. NUMBER OF PAGES | 19a. NAME OF RESPONSIBLE PERSON |
|---|---|---|---|---|---|
| a. REPORT | b. ABSTRACT | c. THIS PAGE | | | USAMRMC |
| U | U | U | UU | 13 | 19b. TELEPHONE NUMBER *(include area code)* |

## Table of Contents

**Page**

## 1.1. Introduction

Tumor microenvironment is as important to the development of the malignant phenotype as the genetic mutations accumulated by cancerous cells over their lifetime [1]. Tumor-associated fibroblasts (TAFs), which express the serine protease fibroblast activation protein alpha (FAP), are up-regulated in the tumor stroma in 90% of all epithelial cancers including prostate cancer (PCa) [2-10]. **This proposal seeks to utilize FAP expression on TAFs within the tumor stroma for the diagnostic imaging of PCa using novel radiopharmaceuticals and innovative multimodal imaging platforms.** We have developed peptides that are specific for the FAP active site, conjugated them to the cross-bridged macrocycle 4,11-bis(carboxymethyl)-1,4,8,11-tetraazabicyclo[6.6.2]hexadecane (CB-TE2A), and radiolabeled them with $^{64}$Cu, which has favorable decay characteristics ($t_{½}$ = 12.7 h; $\beta^+$: 19%; $E_{\beta+\ max}$, 0.656 MeV; EC: 41%; $\beta^-$: 40%) for PET imaging [11]. This report summarizes the experiments completed and the progress made during the current funding period.

## 1.2. Body

Despite the important role of FAP in tumor biology, PCa and cancer therapy, there remains a dearth of molecular probes designed to detect and quantify FAP *in vivo*. A peptide-based, diagnostic PET agent that can detect FAP *in vivo* would be of great value to the medical community since PET is superior to SPECT in terms of sensitivity and resolution and it is not influenced by the same limitations, which hinder optical imaging methods [12]. Furthermore, peptide based agents demonstrate greater design flexibility, greater tolerance to diverse reaction conditions during preparation and better biokinetic and clearance properties when compared to antibodies, which can result in enhanced contrast and reduced patient burden during imaging. Moreover, agents designed to exploit FAP expression would serve as non-invasive imaging agents for the early detection of cancer, the stratification of patients for FAP therapy and the monitoring of response to treatment [13].

(1) Lys(R)-**Thr-Ser-Gly-Pro-Asn**-Glu-$CONH_2$
(2) Lys(R)-**Thr-Ala-Gly-Pro-Asn**-Glu-$CONH_2$
(3) Lys(R)-**Ala-Ala-Gly-Pro-Asn**-Glu-$CONH_2$
(4) Lys(R)-**Thr-Ser-Gly-Pro-Ser**-Glu-$CONH_2$

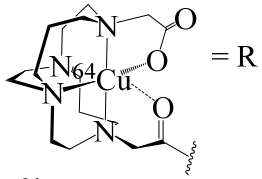


**$^{64}$Cu-CB-TE2A**

(5) Lys(R)-**Thr-Ser-Gly-Pro-Asn**-Glu(R')
(6) Lys(R)-**Thr-Ala-Gly-Pro-Asn**-Glu(R')
(7) Lys(R)-**Ala-Ala-Gly-Pro-Asn**-Glu(R')
(8) Lys(R)-**Thr-Ser-Gly-Pro-Ser**-Glu(R')

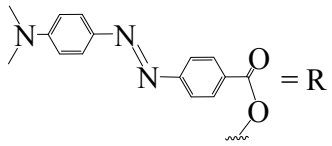


DABCYL

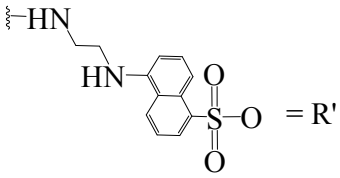


EDANS

**Figure 1. Compounds and conjugates synthesized during the funding period.** Conjugates 1-4 will be radiolabeled with copper-64, while conjugates 5-8 will be used in plate based FRET assays to determine the specificity of each ligand for the FAP active site. All ligands have been synthesized using standard Fmoc based, solid phase peptide synthesis.

During the current funding period, research focused on the synthesis of conjugates **1-4** using standard Fmoc solid phase peptide chemistry. While peptide synthesis proceeded smoothly, coupling of the CB-TE2A chelator to each peptide proved challenging due to the low reactivity of the chelator's carboxylic acid based pendant arms. Reaction with excess chelator for an extended period finally afforded 5 mg of each product in 95% purity. Additionally 5 mg quantities of conjugates **5-8,** which contain the quencher, (4-((4-dimethylaminophenyl)azo)benzoic acid) (DABCYL) and the fluorophore (5-((2-aminoethyl)amino)naphthalene-1-sulfonic acid) (EDANS), each fluorescent cleavage product, and the positive and negative control peptides (RK(DABCYL)TS**GP**NQEQE(EDANS)R), (RK(DABCYL)TS**GG**NQEQE(EDANS)R), respectively have also been prepared. Now that peptide synthesis has been completed current efforts are focused on validating the plate based FRET assay needed to evaluate each peptide sequence as a substrate for the FAP active site using both the positive and negative control peptides. Additionally, standard curves of each fluorescent product are being developed in order to convert relative fluorescence units into moles of product, and it is anticipated that all studies relating to the plate based FRET assay will be completed during the first three months of the second funding period.

A second research objective during the current funding period has been to optimize radiolabeling conditions including time, temperature and pH, for conjugates **1-4**. An optimized radiolabeling scheme is presented in Figure 2-A, which depicts conjugate **1** and is representative of all 4 conjugates. Reaction of each conjugate in ammonium acetate buffer under basic conditions for 30 minutes at 95ºC yields the desired radiolabeled conjugate in high radiochemical purity (Figure 2-B and Figure 2-C). High temperature and basic conditions are necessary due to the proton sponge behavior of the cross-bridged macrocycle[14,15]. Radiolabeled conjugates can be prepared with a specific activity of 37 MBq (1 mCi)/µg, which is consistent with the specific activity of other $^{64}$Cu-CB-TE2A conjugates that have been reported in the literature and used in *in vitro* and *in vivo* studies [16-19]. Importantly, optimization of these parameters has eliminated the need for solid phase purification, and reduced the production time of these radiopharmaceuticals to 30 minutes. Additionally, we have evaluated the stability of each conjugate overt time in saline and in human serum. Figure 2-D depicts the stability of **$^{64}$Cu-1** in saline. In this system, unchelated or transchelated $^{64}$Cu remains at the origin while the intact conjugate moves toward the solvent front. As can be observed, **$^{64}$Cu-1** is remarkably stable even after 24 h and reflects the kinetically inert nature of the $^{64}$Cu-CB-TE2A complex [15]. Similar stability results are observed in human serum (See Appendix A, Figure 1.).

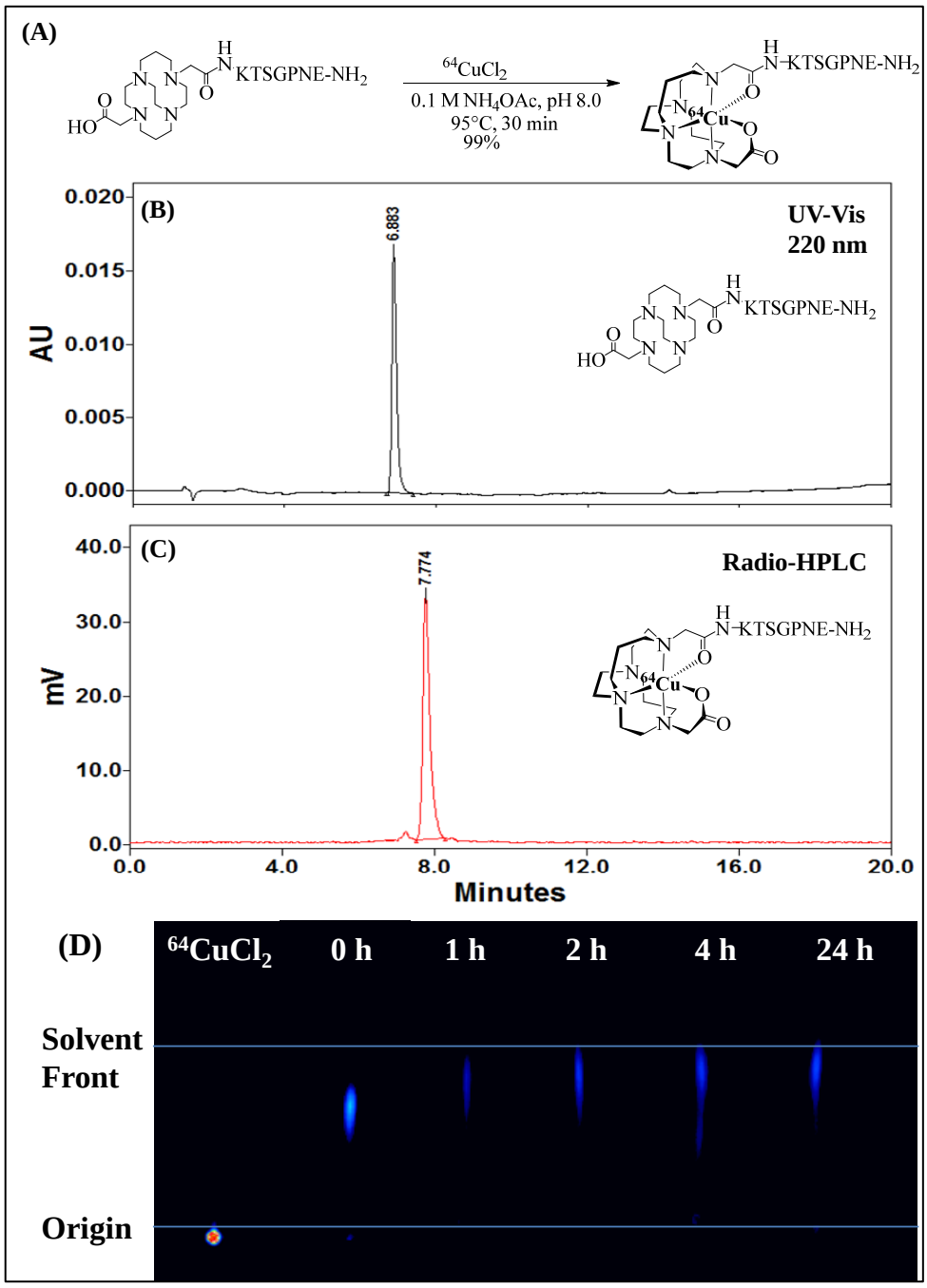


**Figure 2. Radiochemistry and *in vitro* Stability of $^{64}$Cu-1. (A)** Radiochemistry scheme for **$^{64}$Cu-1**. **$^{64}$Cu-1** is prepared in high radiochemical purity and specific activity under basic conditions and at elevated temperature. (B) UV-Vis chromatogram of conjugate **1**. (C) Radio-chromatogram of **$^{64}$Cu-1**. The retention time of the radiotracer differs from that of the non-radioactive ligand and is expected after $^{64}$Cu complexation. (D) *In vitro* stability of **$^{64}$Cu-1** in saline. In this mobile/stationary phase radio-TLC system, any unchelated $^{64}$Cu remains at the origin while the **$^{64}$Cu-1** moves with the solvent front. These results are representative of all $^{64}$Cu radiopharmaceuticals (1-4).

Very few endogenous cell lines exhibit stable FAP expression [20,21]. Thus, a third objective during the current funding period was to create reporter based cell lines with stable FAP expression. While several malignant cell lines express FAP, we sought to engineer our own cell lines in order to 1) create stable FAP expression, 2) minimize complications such as cellular heterogeneity and variable protein

expression, which are often associated with a tumor derived from an un-engineered malignant cell line, and 3) create a model system against which the radiolabeled conjugates could be tested *in vitro* and *in vivo* [22]. Our research focused on developing a eGFP+ FAP+ NIH3T3 mouse fibroblast line and an eGFP+ FAP+ BJ cell line, which is derived from normal human foreskin. In parallel, attempts were made to develop both lines using plasmids containing either the fusion gene of eGFP/FAP or a cotransfection strategy was employed whereby separate plasmids containing eGFP or FAP genes were cotransfected into each cell line (See Appendix B, Figure 1). Initial results using transfection protocols requiring $CaPO_3$ were negative due to low transfection efficiencies, which led the research team to attempt transfections using commercially available transfection kits [23]. While the use of these kits increased transfection efficiencies dramatically, many of the resulting cells demonstrated only transient expression of eGFP or FAP and loss of expression over the course of the selection process. Further progress was retarded by the slow doubling time of the cells in culture or the low enrichment of eGFP+/FAP+ cells after each round of selection (See Appendix B, Table 1.). Despite these setbacks, several cell lines have been prepared by both methods and have been confirmed for FAP and eGFP expression using immunohistochemistry and FACS. Figure 3 represents the results of immunohistochemistry with 3T3 cells stably transfected with the plasmid containing the eGFP/FAP fusion gene. Although eGFP expression appears low, FAP expression is corroborated by anti-FAP antibody staining (Figure 3F, 3H). Mock transfected 3T3 cells did not demonstrate significant eGFP or FAP expression (Figure 3B, 3D). Similar results are observed with BJ cells that were transfected using both transfection procedures, and both cell lines are currently in culture. Experiments are planned during the next funding period to implant these cells in animals in order to observe their respective growth characteristics and determine if eGFP and FAP expression are retained once implanted *in vivo*.

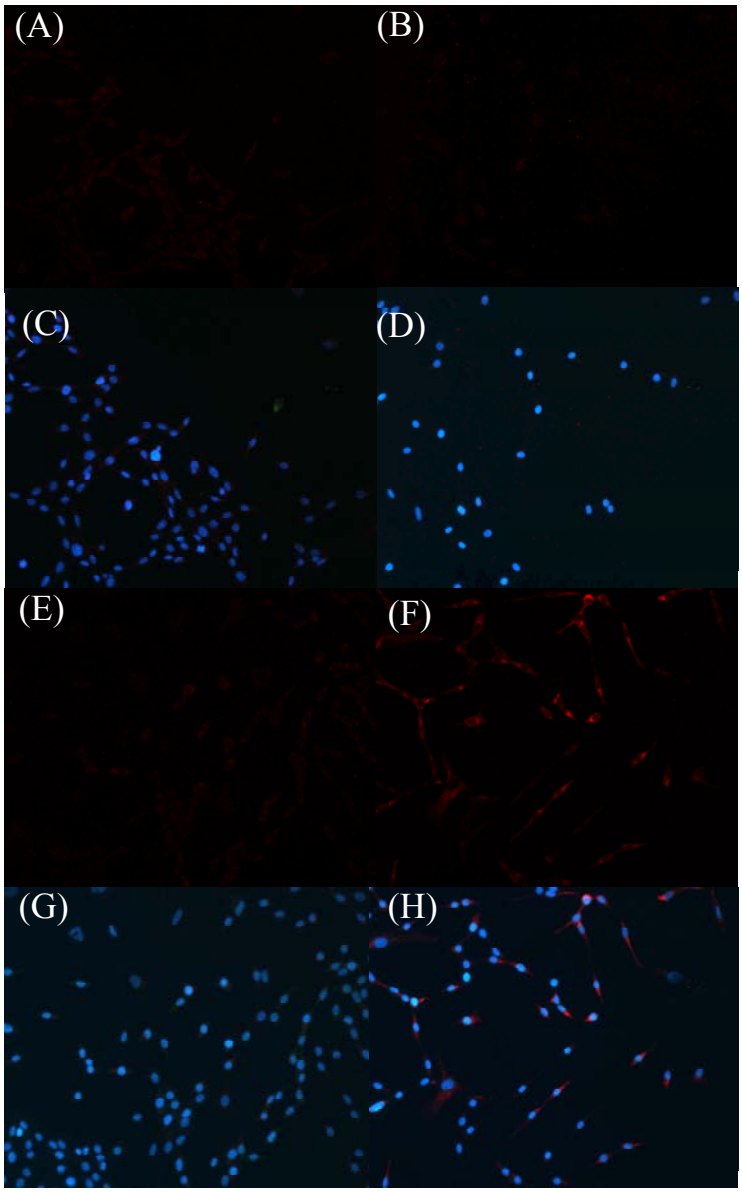


**Figure 3. Development of a Transfected NIH 3T3 Cell Line with Stable FAP Expression.** Panels A, B, C, D represent mock transfected NIH 3T3 cells, while Panels E, F, G, H represent NIH 3T3 cells transfected with the eGFP/FAP fusion plasmid. Cells are stained with 1º IgG control and 2º , anti-IgG mAb conjugated with AlexaFluor 680 (A, E) or 1º anti-FAP mAb and 2º anti-IgG mAb conjugated with AlexaFluor 680 (B, F). Cells are stained with DAPI (C, D, G, H). Strong localization of FAP expression is observed in transfected cells (F, H) while FAP expression is not observed in the mock transfected cells. (B, D).

### 1.3. Key Research Accomplishments

- **SOW Tasks 1, and 2A:** All conjugates (**1-8**), all standards and all positive and negative control peptides have been prepared.
- **SOW Task 3A:** Human and murine cell lines have been created that are observed to express eGFP and FAP.
- **SOW Task 3C:** The radiochemical synthetic conditions needed to incorporate $^{64}Cu$ into conjugates **1-4** have been optimized.

- **SOW Task 3C:** The stability of each conjugate has been evaluated in saline and human serum.

## 1.4. Reportable Outcomes

1. Human and murine cell lines have been created that are observed to express eGFP and FAP.
2. Four new radiopharmaceuticals, which are stable in human serum and are currently being evaluated as FAP substrates, have been prepared for *in vitro* and *in vivo* studies.

## 1.5. Conclusion

Targeting stromal elements such as tumor associated fibroblasts (TAFs) within the tumor microenvironment represents a novel way to detect and image PCa. TAFs express FAP, which is strictly regulated to the surface of TAFs found in the tumor stroma, but is not observed on PCa cells, normal fibroblasts or other benign tissues. Despite the important role of FAP in tumor biology, PCa and cancer therapy, there remains a dearth of molecular probes designed to detect and quantify FAP *in vivo.* In the current funding period, our research has sought to create a foundation for future experiments that probe the importance of TAFs in prostate cancer tumor development using novel radiopharmaceuticals and innovative multimodal imaging platforms. Importantly, we have created two fibroblast cell lines that can be used to evaluate novel radiopharmaceuticals that target FAP. Finally, we have created the first PET based radiotracers that have been designed to target FAP in the prostate tumor stroma. If successful, the development of these agents will provide a novel way of non-invasively imaging PCa. Equipped with this technology, physicians will be able to improve diagnostic accuracy, enhance therapeutic planning in an effort to decrease suffering and improve patient survival.

## 1.6. References


1. Stasinopoulos I, Penet M-F, Chen Z, Kakkad S, Glunde K, Bhujwalla ZM. Exploiting the tumor microenvironment for theranostic imaging. *NMR Biomed*. 2011;24:636-647
2. Tuxhorn JA, Ayala GE, Smith MJ, Smith VC, Dang TD, Rowley DR. Reactive stroma in human prostate cancer: Induction of myofibroblast phenotype and extracellular matrix remodeling. *Clin Cancer Res*. 2002;8:2912-2923
3. Tuxhorn JA, McAlhany SJ, Dang TD, Ayala GE, Rowley DR. Stromal cells promote angiogenesis and growth of human prostate tumors in a differential reactive stroma (drs) xenograft model. *Cancer Res*. 2002;62:3298-3307
4. Bhowmick NA, Neilson EG, Moses HL. Stromal fibroblasts in cancer initiation and progression. *Nature*. 2004;432:332-337
5. Lee KN, Jackson KW, Christiansen VJ, Lee CS, Chun JG, McKee PA. Antiplasmin-cleaving enzyme is a soluble form of fibroblast activation protein. *Blood*. 2006;107:1397-1404
6. Edosada CY, Quan C, Tran T, Pham V, Wiesmann C, Fairbrother W, Wolf BB. Peptide substrate profiling defines fibroblast activation protein as an endopeptidase of strict gly(2)-pro(1)-cleaving specificity. *FEBS Lett*. 2006;580:1581-1586
7. Edosada CY, Quan C, Wiesmann C, Tran T, Sutherlin D, Reynolds M, Elliott JM, Raab H, Fairbrother W, Wolf BB. Selective inhibition of fibroblast activation protein protease based on dipeptide substrate specificity. *J Biol Chem*. 2006;281:7437-7444
8. Aggarwal S, Brennen WN, Kole TP, Schneider E, Topaloglu O, Yates M, Cotter RJ, Denmeade SR. Fibroblast activation protein peptide substrates identified from human collagen i derived gelatin cleavage sites. *Biochemistry*. 2008;47:1076-1086
9. Scanlan MJ, Raj BK, Calvo B, Garin-Chesa P, Sanz-Moncasi MP, Healey JH, Old LJ, Rettig WJ. Molecular cloning of fibroblast activation protein alpha, a member of the serine protease family

selectively expressed in stromal fibroblasts of epithelial cancers. *Proc Natl Acad Sci U S A*. 1994;91:5657-5661

10. Micke P, Ostman A. Tumour-stroma interaction: Cancer-associated fibroblasts as novel targets in anti-cancer therapy? *Lung Cancer*. 2004;45 Suppl 2:S163-175
11. Shokeen M, Wadas TJ. The development of copper radiopharmaceuticals for imaging and therapy. *Med. Chem.* 2011;7:413-429
12. Frangioni JV. New technologies for human cancer imaging. *J Clin Oncol*. 2008;26:4012-4021
13. Li J, Chen K, Liu H, Cheng K, Yang M, Zhang J, Cheng J, Zhang Y, Cheng Z. An activatable near infrared fluorescent probe for in vivo imaging of fibroblast activation protein-alpha. *Bioconjug Chem*. 2012
14. Wadas TJ, Anderson CJ. Radiolabeling of teta- and cb-te2a-conjugated peptides with copper-64. *Nat. Protoc.* 2006;1:3062-3068
15. Wadas TJ, Wong EH, Weisman GR, Anderson CJ. Coordinating radiometals of copper, gallium, indium, yttrium, and zirconium for pet and spect imaging of disease. *Chem. Rev.* 2010;110:2858-2902
16. Wadas TJ, Deng H, Sprague JE, Zheleznyak A, Weilbaecher KN, Anderson CJ. Targeting the alphavbeta3 integrin for small-animal pet/ct of osteolytic bone metastases. *J Nucl Med*. 2009;50:1873-1880
17. Wadas TJ, Eiblmaier M, Zheleznyak A, Sherman CD, Ferdani R, Liang K, Achilefu S, Anderson CJ. Preparation and biological evaluation of 64cu-cb-te2a-sst2-ant, a somatostatin antagonist for pet imaging of somatostatin receptor-positive tumors. *J. Nucl. Med.* 2008;49:1819-1827
18. Wei L, Ye Y, Wadas TJ, Lewis JS, Welch MJ, Achilefu S, Anderson CJ. 64cu-labeled cb-te2a and diamsar-conjugated rgd peptide analogs for targeting angiogenesis: Comparison of their biological activity. *Nucl. Med. Biol.* 2009;36:277-285
19. Zheleznyak A, Wadas TJ, Sherman CD, Wilson JM, Kostenuik PJ, Weilbaecher KN, Anderson CJ. Integrin α(v)β (3) as a pet imaging biomarker for osteoclast number in mouse models of negative and positive osteoclast regulation. *Mol Imaging Biol*. 2012;14:500-508

20. Rettig WJ, Garin-Chesa P, Beresford HR, Oettgen HF, Melamed MR, Old LJ. Cell-surface glycoproteins of human sarcomas: Differential expression in normal and malignant tissues and cultured cells. *Proc Natl Acad Sci U S A*. 1988;85:3110-3114

21. Rettig WJ, Grzeschik KH, Yenamandra AK, Garcia E, Old LJ. Definition of selectable cell surface markers for human chromosomes and chromosome segments in rodent-human hybrids. *Somat Cell Mol Genet*. 1988;14:223-231

22. Moiola C, De LP, Gardner K, Vazquez E, De SA. Cyclin t1 overexpression induces malignant transformation and tumor growth. *Cell Cycle*. 2010;9:3119-3126

23. Bitsika V, Roubelakis MG, Zagoura D, Trohatou O, Makridakis M, Pappa KI, Marini FC, Vlahou A, Anagnou NP. Human amniotic fluid-derived mesenchymal stem cells as therapeutic vehicles: A novel approach for the treatment of bladder cancer. *Stem Cells Dev*. 2012;21:1097-1111

## 2.0. Appendix A

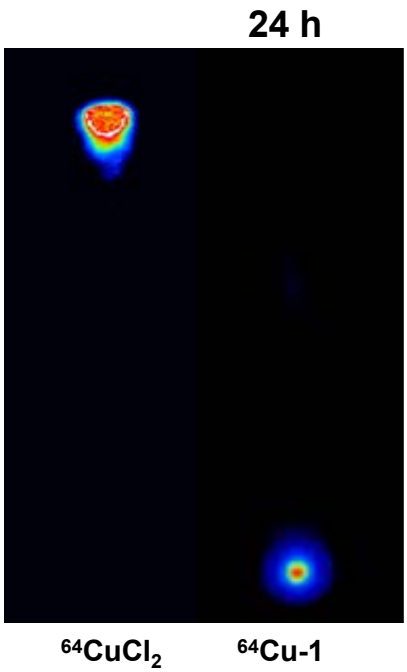


**Figure 1. *In vitro* Serum Stability of $^{64}$Cu-1.** The radiotracer, **$^{64}$Cu-1** is incubated in the presence of human serum at physiologic temperature. Aliquots are withdrawn and spotted on ITLC paper and developed in saline. $^{64}CuCl_2$ is included as a positive control for transchelation. In this radio-TLC system, any $^{64}$Cu that is transchelated to serum proteins migrates with the solvent front. **$^{64}$Cu-1** does not undergo transchelation even after 24 h in human serum at physiologic temperature.

## 2.1. Appendix B

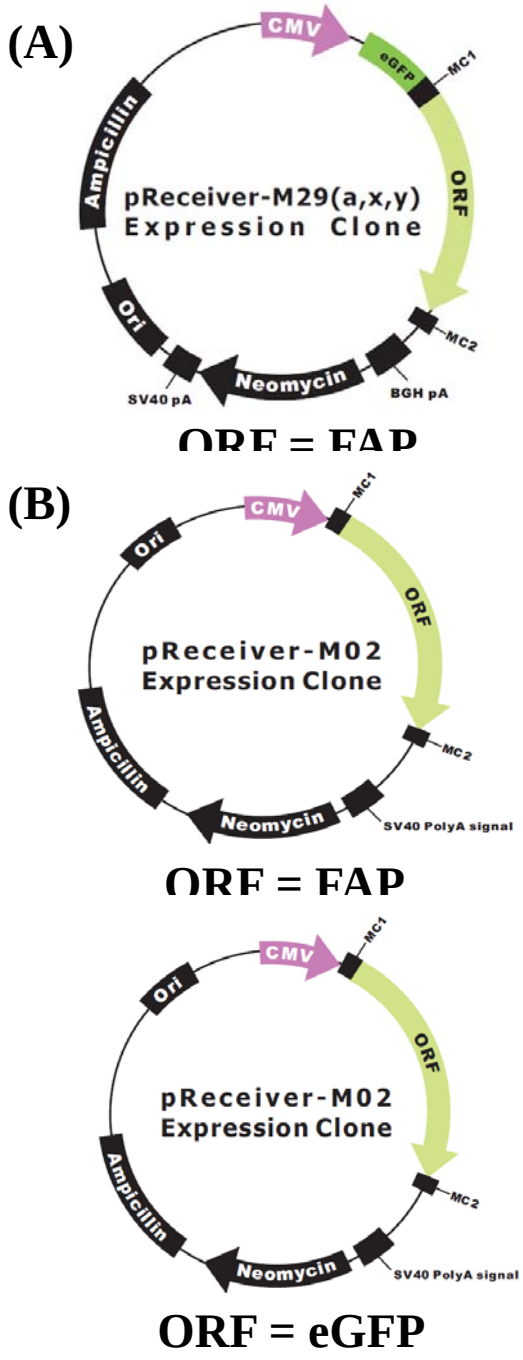


**Figure 1. Plasmids Used to Develop Cell Lines with Stable FAP and eGFP Expression.** Two strategies were employed and included the use of (A) a plasmid containing a fusion gene of eGFP and FAP or (B) a cotransfection strategy. All plasmids were purchased from GeneCopoeia (Rockville, MD).

**Table 1. Selection Efficiency of Transfected 3T3 and BJ Cells**

| | code | transfection | 1th sorting | 2sd sorting | 3rd sorting | 4th sorting |
|---|---|---|---|---|---|---|
| 3T3 | T3 | FAP/eGFP | No cells | | | |
| | T4 | FAP/eGFP | No cells | | | |
| | T5 | FAP/eGFP | 0.02% | No cells | | |
| | T6 | FAP/eGFP | 0.8% | 0.08% | 2.9% | |
| | P2T1 1/10 | 1xFAP vs1/10 eGFP | 2.8% | 7.5% | | |
| | P2T1 1/20 | 1xFAP vs1/20 eGFP | 2.1% | | | |
| | T7 | FAP/eGFP | 0.01% | 6% | | |
| | P2T2 1/20 | 1xFAP vs1/20 eGFP | 0.5% | | | |

| | code | transfection | 1th sorting | 2sd sorting | 3rd sorting | 4th sorting |
|---|---|---|---|---|---|---|
| BJ | T3 | FAP/eGFP | 0.028% | 0.18% | 2.8% | 30% |
| | T4 | FAP/eGFP | 0.18% | 0.3% | 0.28% | 25% |
| | T5 | FAP/eGFP | No cells | | | |
| | P2T1 1/10 | 1xFAP vs1/10 eGFP | 1.1% | | | |
| | P2T1 1/20 | 1xFAP vs1/20 eGFP | 0.6% | | | |
| | P2T2 1/10 | 1xFAP vs1/20 eGFP | 5.7% | | | |

Code beginning with "T" refers to transfection with plasmid containing fusion FAP/eGFP gene.
Code beginning with "P" refers to cotransfection. Once sorting produced a population with at least 5% positive cells, additional rounds of selection using FACS was discontinued.